Available online at www.sciencedirect.com
SCIENCE DIRECT®
Journal of Solid State Chemistry 175 (2003) 380–383
JOURNAL OF SOLID STATE CHEMISTRY
http://elsevier.com/locate/jssc

Synergetic theoretical and experimental structure determination of nanocrystalline materials: study of $LiMoS_2$

X. Rocquefelte,* I. Bouessay, F. Boucher, P. Gressier, and G. Ouvrard

Laboratoire de Chimie des Solides, Institut des Matériaux Jean Rouxel, UMR 6502 Université de Nantes – CNRS, 2 rue de la Houssinière, BP 32229, 44322 Nantes Cedex 03, France

Received 12 February 2003; received in revised form 22 May 2003; accepted 2 June 2003

Abstract

A combined approach is proposed to solve the structure of badly crystallized materials. It couples poor quality powder X-ray diagram (XRD) and XRD simulation deduced from first-principle geometry optimization. It is used to completely solve the $LiMoS_2$ structure.

Keywords: $LiMoS_2$; DFT; XRD simulation; Poorly crystallized materials

An accurate knowledge of the atomic structure appears to be a really difficult task in an increasing number of cases. This originates, particularly, in the expansion of soft-chemistry route synthesis and the increased importance of nanomaterials [1]. It is usual to encounter materials for which the atomic order is limited to the nanometer length scale, by small size or disorder effect. In such a case, where the coherence length is very short, traditional crystallography fails in the structure determination, and local techniques give only partial structural information, which is highly dependent of the resolution of the method (XAS, NMR, electron diffraction). It is therefore important to find a new pertinent combination of such tools in order to determine the complete structure of such materials.

In the present paper, we propose to combine these experiments with theory to completely solve the structural arrangement of such phases. We show, with the example of $LiMoS_2$, that periodic boundary conditions based methods can be used to determine the structure of poorly crystalline and nanocrystalline materials. This study particularly put in evidence that, in the case of $LiMoS_2$, the nanoscale refers to the crystallite size without changing drastically the atomic arrangement.

$LiMoS_2$ is an important precursor of stable MoS_2 colloids used to prepare a variety of lamellar nanocomposites [2]. Those intercalation compounds exhibit many different properties and related applications, as catalysis, magnetism, tribology, etc. This compound can be obtained from lithium insertion into MoS_2. Unlike the pristine phase, $LiMoS_2$ is not well ordered, and its powder X-ray diagram (XRD) exhibits broad Bragg peaks (top of Fig. 1). This is the signature of a short structural coherence length, of about 50 Å [3]. Many people tried to solve the structure in using experimental approaches. From the X-ray diffraction powder data, an hexagonal cell was first proposed [4] and a more precise study reveals a distortion to a monoclinic or triclinic symmetry inducing a $(2\mathbf{a} \times 2\mathbf{a})$ superstructure [5], **a** standing for the undistorted hexagonal lattice parameter. Nevertheless, the authors have not been able to refine the atomic positions. An important step was the discovery of molybdenum clusters by XAS [6]. Recently, atomic pair distribution function (PDF) experiments [7] have been used in order to completely solve the structure [3]. The so-obtained cell parameters (Exp2 in Table 1) differ significantly from those previously deduced from X-ray diffraction [5] (Exp1 in Table 1): a larger **a** parameter (+2.4%) and a smaller **b** parameter (−5.4%) are found. These observations show that the structure

*Corresponding author. Fax: 33-2-40-37-39-95.
E-mail address: xavier.rocquefelte@cnrs-imn.fr (X. Rocquefelte).

0022-4596/03/$ - see front matter © 2003 Elsevier Inc. All rights reserved.
doi:10.1016/S0022-4596(03)00330-X

determination of the nanocrystalline material $LiMoS_2$ is not trivial. Depending on the experimental technique, results can be significantly different.

In a previous work, on the basis of experimental data [8,9], we used first-principle calculations to propose a structural model of $LiMoS_2$ [10]. The optimized structure has a triclinic symmetry (space group $P\bar{1}$), and the cell parameters are in good agreement with the XRD ones (Opt1 in Table 1). The obtained in-plane atomic arrangement exhibits a distortion inside the Mo plane leading to the formation of a $(2\mathbf{a} \times 2\mathbf{a})$ superstructure. This distortion is due to the occurrence of short Mo–Mo distances in agreement with the formation of Mo diamond chain clusters. This local arrangement has been confirmed by the PDF techniques. Therefore, while PDF is not very accurate for the cell parameter determination, it appears as a performing technique to propose local atomic arrangement.

In the paper, using a back and forth procedure, we combine the results of first-principle calculations and simulation of poorly resolved X-ray diagrams, to completely solve the atomic arrangement. Furthermore, we will compare our results with a recently obtained XRD pattern of a highly crystalline $LiMoS_2$ and another simulation corresponding to the atomic structure proposed by Petkov et al. [3].

In our previous theoretical study, different models have been proposed for the anionic packings. In order to check them, we did the corresponding XRD simulation using the PowderCell program [11]. Pseudo-Voigt profile function has been used to reproduce the experimental peak broadening. This investigation was motivated by the existence of many polytypes in the lamellar dichalcogenides family. For instance, two natural MoS_2 forms are known: 2Hb (AABB sulfur stacking) and 3R (AABBCC sulfur stacking). In the case of $LiMoS_2$ and with respect to the above-described in-plane ordering, four hexagonal close packings (ABAB) and four face-centered cubic ones (ABCABC) have to be considered (Fig. 1). A comparison between the simulations and the experimental $LiMoS_2$ powder X-ray diagram ($LiMoS_2$ was obtained by reacting pristine MoS_2 with excess of *n*-BuLi) is shown in Fig. 1. The differences between the models are clearly revealed in the simulated diagrams, showing that such simulations are perfectly able to discriminate between various hypotheses. In agreement with the results of total energy calculations [10], none of the four ABCABC models (from (a) to (d)) allows a correct simulation of the experimental pattern. Particularly, a high disagreement is found for the 2θ range from 25° to 50°. On the contrary, a much better agreement with the experimental diagram is observed for all the simulations related to an ABAB sulfur packing. Considering carefully the relative intensities of the strong and the weak peaks, it is clear, however, that the best simulation corresponds to the structure denoted (e) in Fig. 1. Especially, the experimentally observed peaks around 15.5° and 21° disappear gradually in the simulations from (e) to (h). At the same

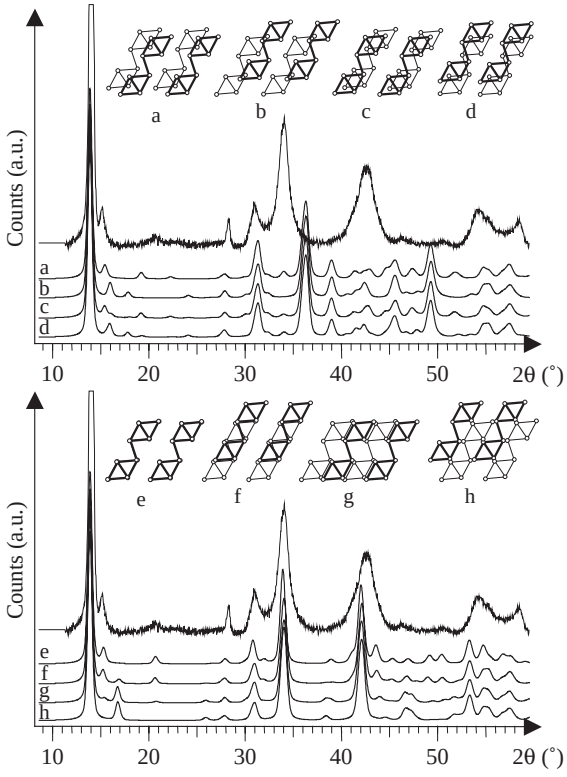

Fig. 1. Structure models and related X-ray diagram simulations compared to the experimental one (on top, "*n*-BuLi synthesis"). ABCABC sulfur stacking patterns from (a) to (d) and ABAB ones from (e) to (h). Only two successive Mo planes are represented.

Table 1
Comparison between $LiMoS_2$ cell parameters obtained in two different experimental studies with our prediction

	a	*b*	*c*	*α*	*β*	*γ*
Exp1 [5]	6.798	6.754	6.292	90.00	90.00	121.20
Exp2 [3]	6.963 [+**2.4**]	6.386 [−**5.4**]	6.250 [−0.7]	88.60	89.07	120.06
Opt1 [10]	6.700 [−1.4]	6.700 [−0.8]	6.390 [+**1.6**]	90.00	90.00	**120.00**
Opt2	6.862 [+0.9]	6.812 [+0.9]	6.296 [+0.1]	89.97	90.28	121.42

Note. Discrepancies between the values are given in square brackets (in %).

time a new peak, experimentally not observed, grows at about 17°.

Keeping this best (e) model, we performed a new series of calculations in order to carry out a full geometry optimization with complete cell relaxation. We used for this purpose the Vienna Ab initio Simulation Program (VASP) [12–15], a package based on the density functional theory. In this type of calculations, the wave functions are expanded into a plane-wave basis set with a kinetic energy below 340 eV (≈ about 220 plane waves per atom). The VASP package is used with the projector augmented wave (PAW) method of Blöchl [16,17]. The electronic exchange and correlation are treated in the local density approximation (LDA), and corrections are taken into account by the generalized gradient approximation (GGA) exchange and correlation functional of Perdew–Burke–Ernzerhof [18]. The integration in the Brillouin Zone is done by the tetrahedron method corrected by Blöchl [19] on a set of k-points determined by the Monkhorst and Pack scheme [20]. All the optimizations of atomic coordinates and cell parameters are driven by following a conjugated gradient minimization of the total energy scheme (Hellmann–Feynman forces on the atoms and stresses on the unit cell [21]).

The so-obtained cell parameters[1] are now very close to the experimental ones proposed by Mulhern et al. (Opt2 in Table 1). It can be noticed that the **a** and **b** parameters are nearly equal, and no important deviation from 90° is found for α and β angles. Moreover, as experimentally observed, the γ angle value differs significantly from 120° (121.42° in our calculation). Contrary to the very good agreement between X-ray studies and DFT calculations, the cell parameters extracted from PDF experiments are significantly different from the other ones. A comparison of the bond length deduced from the PDF and DFT models with the available experimental data (EXAFS and tabulated values) is given in Table 2. Calculated Mo–S (2.48 Å), Mo–Mo (2.95 Å) and Li–S (2.59 Å) bond lengths agree very well with the experimental values deduced from EXAFS studies (Mo−S = 2.44 Å, Mo−Mo = 2.94 Å) [6] and the tabulated values (Li−S = 2.60 Å) [22]. On the contrary, noticeable differences are observed for the Mo–S (2.57 Å) and Li–S (2.45 Å) bond lengths deduced from PDF experiments, while a good agreement is found for the Mo–Mo distance (2.96 Å).

[1] Atomic coordinates for the optimized structure ($a = 6.862$ Å, $b = 6.812$ Å, $c = 6.296$ Å, $\alpha = 89.97°$, $\beta = 90.28°$, $\gamma = 121.42°$): Mo1: 0.943 0.751 0.504; Mo2 0.492 0.702 0.500; S1 0.656 0.587 0.773; S2 0.183 0.077 0.746; S3 0.678 0.087 0.698; S4 0.153 0.583 0.718; Li1 0.010 0.750 0.022; Li2 0.482 0.772 0.989.

Table 2
Comparison between some mean interatomic distances in $LiMoS_2$

Distances (Å)	Calculated	PDF [3]	Expected [22]	EXAFS data [6]
Li–S	2.59 [2.53–2.67]	2.45 [2.08–3.10]	2.60	—
Mo–S	2.48 [2.37–2.62]	2.57 [2.29–2.83]	2.46	2.44
Mo–Mo	2.95 [2.81–3.06]	2.96 [2.90–3.10]	—	2.94

Value ranges are in squares brackets.

Usually one argument put forward to justify the discrepancy between the different experiments is that the product critically depends on the experimental conditions (reactants, temperature, pressure, etc.). In order to estimate the effect of the route synthesis on the $LiMoS_2$ structure, a parallel study has been recently performed [23]. Depending on the synthesis procedure, different XRD were obtained. Figs. 2a and b exhibit the XRD pattern related n-BuLi [24] and $LiBH_4$ [3] intercalation reactions and Fig. 2c gives the XRD simulation corresponding to a highly crystalline $LiMoS_2$ sample. From Figs. 2a–2c only a narrowing of the peaks is observed. This clearly shows that the only change between the three $LiMoS_2$ products is the crystallite size. The absence of any peak shift indicates that there is no evident structural modifications. This result suggests that the nanometer scale $LiMoS_2$ sample ($LiBH_4$ synthesis) used for PDF measurements has the same structure as the highly crystalline compound except the crystallite size. For that reason we will now focus on the well-defined X-ray pattern (Fig. 2c) in order to compare it with the XRD simulations deduced from the DFT optimization (Fig. 2d) and the PDF experiments (Fig. 2e). A very good agreement is found with DFT simulation. The pattern obtained from the PDF experiments shows many common features with the experimental X-ray diagram, but an important discrepancy is found for the peaks at about 29.5°, 35° and 44.5°.

To summarize, from the above XRD analysis we may expect that the nanocrystalline structure of $LiMoS_2$ is very close to the crystalline one. The first experimental proposition of a full crystallographic structure of $LiMoS_2$ has been done using PDF techniques. However, this method did not allow to obtain accurate cell parameters and atomic positions. For this reason, it appears very promising to combine such experimental approach with first-principle calculations for future studies.

These recent experimental results emphasize the power of our theoretical approach to propose good model structure for poorly crystalline and/or nanocrystalline materials. We have shown that this approach is able to predict many details of the X-ray diagram of a highly crystalline material, without considering any

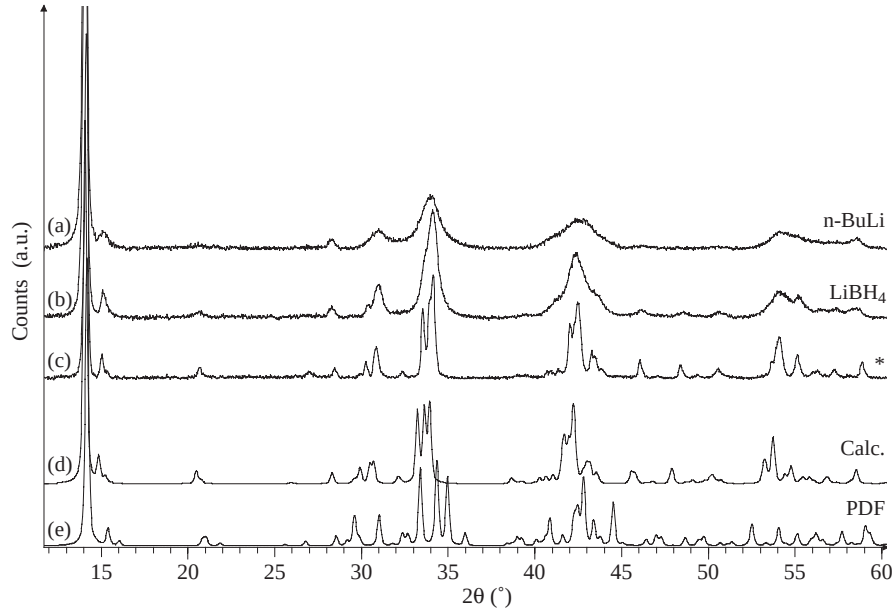

Fig. 2. $LiMoS_2$ XRD diagrams ($CuK_{\alpha 1}$ radiation) corresponding to n-BuLi (a) and $LiBH_4$ (b) intercalation reactions and highly crystallized samples (c), and XRD simulations deduced from DFT calculations (d) and PDF experiments (e).

accurate experimental information. The main benefit of such an approach is the possibility to test models using only scarce experimental information. Then, by optimizing the geometry of hypothetical structures it is possible to fully determine the structure of materials that are poorly crystallized or nanocrystallized. This successful method can probably be applied to many nanostructured phases, providing that there is an available XRD, even of poor quality. It is valid in various domains such as catalysis, fuel cells, and electrochemistry. Such an approach was recently and successfully used in the structural and electrochemical study of $Li_xV_2O_5$ system $(0 \leqslant x \leqslant 3)$. One of the main results is the first-principle structure elucidation of the controversial ω-$Li_3V_2O_5$ phase [25].

References

[1] H. Gleiter, Acta Mater. 48 (2000) 1.
[2] W.M.R. Divigalpitiya, R.F. Frindt, S.R. Morrison, Science 246 (1989) 369.
[3] V. Petkov, S.J.L. Billinge, P. Larson, S.D. Mahanti, T. Vogt, K.K. Rangan, M.G. Kanatzidis, Phys. Rev. B 6509 (2002) NIL_18.
[4] M.A. Py, R.R. Haering, Can. J. Phys. 61 (1983) 76.
[5] P.J. Mulhern, Can. J. Phys. 67 (1989) 1049.
[6] K.E. Dungey, M.D. Curtis, J.E. Penner-Hahn, Chem. Mater. 10 (1998) 2152.
[7] V. Petkov, S.J.L. Billinge, J. Heising, M.G. Kanatzidis, J. Amer. Chem. Soc. 122 (2000) 11571.
[8] J. Heising, M.G. Kanatzidis, J. Amer. Chem. Soc. 121 (1999) 638.
[9] J. Heising, M.G. Kanatzidis, J. Amer. Chem. Soc. 121 (1999) 11720.
[10] X. Rocquefelte, F. Boucher, P. Gressier, G. Ouvrard, P. Blaha, K. Schwarz, Phys. Rev. B 62 (2000) 2397.
[11] W. Kraus, G. Nolze, Powder Cell for Windows, v. 2.3, Berlin, Germany, 1999.
[12] G. Kresse, J. Hafner, Phys. Rev. B 49 (1994) 14251.
[13] G. Kresse, J. Hafner, J. Phys.: Condens. Matter 6 (1994) 8245.
[14] G. Kresse, J. Furthmüller, Comput. Mater. Sci. 6 (1996) 15.
[15] G. Kresse, J. Furthmüller, Phys. Rev. B 54 (1996) 11169.
[16] P.E. Blöchl, Phys. Rev. B 50 (1994) 17953.
[17] G. Kresse, D. Joubert, Phys. Rev. B 59 (1999) 1758.
[18] J.P. Perdew, K. Burke, M. Ernzerhof, Phys. Rev. Lett. 77 (1996) 3865.
[19] P.E. Blöchl, O. Jepsen, O.K. Andersen, Phys. Rev. B 49 (1994) 16223.
[20] H.J. Monkhorst, J.D. Pack, Phys. Rev. B 13 (1976) 5188.
[21] R.P. Feynman, Phys. Rev. 56 (1939) 340.
[22] R.D. Shannon, Structure and Bonding in Crystals, Vol. 1, Academic Press, New York, 1981, p. 53, ISBN 0-12-525102-5.
[23] I. Bouessay, F. Boucher, X. Rocquefelte, P. Gressier, G. Ouvrard, to be published.
[24] M.B. Dines, Mater. Res. Bull. 10 (1975) 287.
[25] X. Rocquefelte, F. Boucher, P. Gressier, G. Ouvrard, Chem. Mater. 15 (2003) 1812.